



## CHAOTIC VIBRATIONS OF CLOSED CYLINDRICAL SHELLS IN A TEMPERATURE FIELD

A. V. KRYSKO\*, J. AWREJCEWICZ†, E. S. KUZNETSOVA  
and V. A. KRYSKO

*Saratov State Technical University,  
Department of Higher Mathematics,  
410054, Saratov, Russia*

*†Technical University of Lodz,  
Department of Automatics and Biomechanics,  
Stefanowskiego 1/15, 90-924 Lodz, Poland*

*\*tak@san.ru*

*†awrejcew@p.lodz.pl*

Received November 29, 2006; Revised July 9, 2007

A closed cylindrical shell with circular cross-section having constant stiffness and density and subjected to sign changeable loading and embedded into a temperature field is analyzed. Both Bubnov–Galerkin (with a higher approximation) and Fourier methods are applied to solve the derived nonlinear nondimensional partial differential equations. Among others, the novel scenario of transition from shell harmonic to chaotic vibrations via the collapse of quasi-periodic vibrations with one independent frequency and Hopf bifurcation is detected, illustrated and discussed. In addition, it is shown how for various intensities of the temperature field (including its absence) the increase of the loading yields qualitative changes in the investigated shell dynamics, and how chaotic zones are transmitted into periodic ones and vice versa.

*Keywords:* Vibrations; chaos; cylindrical shell; temperature field; partial differential equations; Bubnov–Galerkin method; Fourier representation.

### 1. Introduction

In general, the shell (plate) type structural members are nowadays often applied in various fields of engineering including aero-navigation, investigation of both ocean stores and civil engineering [Ross, 1975; Liew *et al.*, 1994], as well as mechatronic devices (for instance, sector-membranes used in pressure sensors). In particular, a very important task of today's engineering is associated with a study of nonlinear vibrations of thin spherical shells and circular cylindrical shells. This is motivated mainly by a rapid development of rocket, ship, train, vehicle and other transport tools construction [Avduyevskiy

*et al.*, 1992; Bakulin *et al.*, 1998]. The fundamental part of a study of nonlinear vibration of shells is focused on geometrical aspects of nonlinearity. The essential contribution to this field is introduced by Thompson and Bishop [1994], Nayfeh and Mook [1979], Benamar [1994], Volmir [1972], Bolotin [1964], and others. Below, we briefly review some aspects of the state-of-the art of nonlinear vibrations of shells. Evensen [1974] was one of the first who critically reviewed state-of-the art of the mentioned topic including the results published in the years 1955–1971. On the other hand, although the monograph by Leissa [1973] includes the overview

of over 500 references dedicated mainly to dynamics of circular cylindrical shells, only 24 of them deal with nonlinear shell dynamics.

Paidoussis and Li [1992] studied chaotic dynamics of heat exchanger tubes which had an impact on the generally loose baffle plates. It was shown that for a sufficient flow velocity chaos appeared and a negatively damped impact oscillator was used to understand the system behavior.

Yang and Sethna [1992] studied nonlinear flexural vibrations of nearly square plate being periodically excited with forces normal to the mid-plane of the plate. Dynamics consisting of anti-symmetric or mixed modes occurred. The Hopf bifurcation produced the amplitude-modulated traveling waves with jerky motions. Global chaotic phenomena were observed.

A homogeneous fully clamped rectangular plate subjected to spatially thermal loads and narrow-band acoustic excitation was studied by Murphy *et al.* [1996]. Time series power spectra, autocorrelation functions, spatial dimension and temporal complexity were applied to characterize the occurring chaotic orbits.

Subharmonic resonance of a rectangular plate with uniform stretching when two distinct linear modes are near one-to-one internal resonance was studied by Chang *et al.* [1997]. It was shown via an averaging procedure that the plate could exhibit harmonic and subharmonic motions in the directly excited spatial mode or subharmonic motions in which both the internally resonant modes appeared. A period-doubling route to chaos was shown.

Sun and Zhang [2001] used chaos and fractal theories to study dynamic buckling of viscoelastic plates. A nonlinear integral-differential dynamic equation was reduced to an autonomous four-dimensional dynamic system. Lyapunov spectra and fractal dimensions of strange attractors were reported.

The nonlinear mathematical theory of perforated viscoelastic thin plates using both Kármán hypotheses and Boltzmann's constitutive law of linear viscoelastic materials was derived by Cheng and Fan [2001]. In particular, the nonlinear dynamic stability of a viscoelastic angular plate was studied, and a novel method of Lyapunov exponent spectrum estimation was proposed.

Lai *et al.* [2002] used fractal dimension and the maximum Lyapunov exponent to study large deflections of a simply supported rectangular plate. Fourier spectra, state-space plots, Poincaré maps

and bifurcation diagrams were computed. Various bifurcations were detected and their links to chaotic orbits occurrence were discussed.

Nonlinear equations governing dynamics of Timoshenko's viscoelastic thick plates with damage were derived and studied by Sheng and Cheng [2004]. The influences of load, geometry and material parameters on the dynamic plate behavior were investigated by the Galerkin approach.

Xiao *et al.* [in press] derived nonlinear equations of motion for the rectangular moderately thick plates with a transverse surface penetrating crack on an elastic foundation subject to periodic load action. Bifurcational and chaotic behavior of such plates were studied using the Galerkin and Runge-Kutta integration methods.

Ribeiro and Duarte [2006] studied geometrically nonlinear dynamics of composite laminated plates. The existence of chaos was confirmed by calculation of the largest Lyapunov exponent.

Guo and Mei [2006] showed how the use of aeroelastic modes could reduce drastically the number of coupled nonlinear modal equations for the large amplitude nonlinear panel flutter studied at an arbitrary yawed supersonic flow angle and elevated temperatures. Periodic and chaotic dynamics of the panel were reported.

Ribeiro [2007] studied the chaotic behavior of geometrically nonlinear vibrations of linear elastic and isotropic plates under the combined effect of thermal fields and mechanical excitations. Newmark's implicit time integration method was applied to solve the governing equations in the time domain.

Raouf and Nayfeh [1990] applied a numerical-perturbation approach to study the axisymmetric dynamic vibrations of closed spherical shells subjected to external harmonic excitation with a frequency near one of the natural frequencies of a flexural mode in the presence of a two-to-one auto-parametric resonance between the excited mode and a lower flexural mode. The limit cycles which appeared after Hopf bifurcation underwent pitchfork bifurcation and a cascade of period-doubling bifurcations leading to chaos. Also the subcritical Hopf bifurcation was illustrated, and a cyclic-fold bifurcation yielding chaos was reported, among others.

Popov *et al.* [2001] studied numerically internal auto-parametric instabilities in the free non-linear vibrations of a cylindrical shell. Regular and chaotic behavior of two-modes interaction was analyzed

with emphasis put on energy transfer between the modes.

Soliman and Goncalves [2003] investigated the axisymmetric chaotic dynamic behavior and snap-through buckling of thin elastic shallow spherical shells under harmonic excitation. Both Galerkin and Fourier–Bessel approaches were applied to reduce the partial differential equations to a finite degrees-of-freedom system. Steady-state and transient stability boundaries were presented and the vertical load conditions were determined.

A shallow cylindrical shell under gravity and periodic acceleration and possessing concentrated mass was studied by Nagai *et al.* [2004]. The Galerkin method was used to reduce the problem of ordinary differential equations. The influence of mass value on the chaotic dynamics of the system was investigated as well.

Amabili [2005] studied large vibrations of doubly curved shallow shells with a rectangular base, simply supported at the four edges and subjected to harmonic excitation normal to the surface in the spectral neighborhood of the fundamental mode. Donnell’s and Novozhilov’s shell theories were used to compute the elastic strain energy. Shell stability under static and dynamic loads was studied, both Lyapunov exponents and dimensions were computed, and snap-through instability, subharmonic resonance, as well as the period-doubling routes to chaos were illustrated and discussed.

Pellicano and Amabili [2006] studied dynamic stability of circular cylindrical shells subjected to static and dynamic axial loads. Chaotic dynamics of precompressed shell within Donnell’s and Sanders–Koiter’s theorems was illustrated.

Although Amabili *et al.* [1998] claimed that the full overview of the state-of-the art of nonlinear dynamics of shells embedded in vacuum and/or in a fluid is carried out, it seems that it concerns only the closed circular cylindrical shells and hence omits other configurations of shell systems. In addition, the mentioned mechanical objects are studied mainly through a rough one degree-of-freedom approximation, which is far from the recent engineering expectations.

We illustrate how geometrical nonlinearity provokes a qualitatively novel behavior of nonlinear dynamics of shells which cannot be predicted and exhibited by the linear shells’ theory. Note that Awrejcewicz and Krysko [2003a, 2003b] and Awrejcewicz *et al.* [2005, 2007] dealt with nonlinear dynamics of arbitrary geometry of shells, where

high-order approximation of shell dynamics is taken to achieve almost infinite dimension of the real problem.

After the Challenger accident a rigorous and highly accurate nonlinear analysis of thin-walled structures was highly required. A new design of fuel containers is required, and therefore a rigorous analysis of shells embedded into a temperature field is needed.

In this work the Bubnov–Galerkin method in higher approximations and in the Fourier representation is applied. The Bubnov–Galerkin procedure in the form proposed by Vlasov is used. In particular, the influence of a temperature field on the shell dynamics is studied.

The aim of the paper is not a full and multi-lateral presentation of the problem under investigation, but an attempt of showing the simplicity of realization and effectiveness of the Bubnov–Galerkin method applied to the theoretical problems of plates and shells.

## 2. Formulation of the Problem

In the frame of the nonlinear classical theory of shallow shells a closed cylindrical shell with circular cross-section and of finite length with both constant stiffness and density subjected to sign-changeable loading and embedded into the temperature field is studied. The system of coordinates with the  $x$ -axis coinciding with longitudinal coordinate, the  $y$ -axis coinciding with a circular coordinate, as well as the  $z$ -axis directed along a normal to the mean surface is introduced (Fig. 1). The cylindrical shell as a 3D object  $\Omega$  is defined in the following way in the given system of coordinates:  $\Omega = \{x, y, z | (x, y) \in [0; L] \times [0; 2\pi], -h \leq z \leq h\}$ .

The system of equations governing shell dynamics is given in the following nondimensional form [Volmir, 1963]:

$$\left\{ \frac{1}{12(1-\nu^2)} \left[ \lambda^{-2} \frac{\partial^4 w}{\partial x^4} + 2 \frac{\partial^4 w}{\partial x^2 \partial y^2} + \lambda^2 \frac{\partial^4 w}{\partial y^4} \right] - L(w, F) - k_y \frac{\partial^2 F}{\partial x^2} - \frac{\partial^2 w}{\partial t^2} - \varepsilon \frac{\partial w}{\partial t} - \frac{1}{12(1-\nu^2)} \left( \lambda^{-1} \frac{\partial^2 M_t}{\partial x^2} + \lambda \frac{\partial^2 M_t}{\partial y^2} \right) \right\} + k_y^2 q(x, y, t) = 0,$$

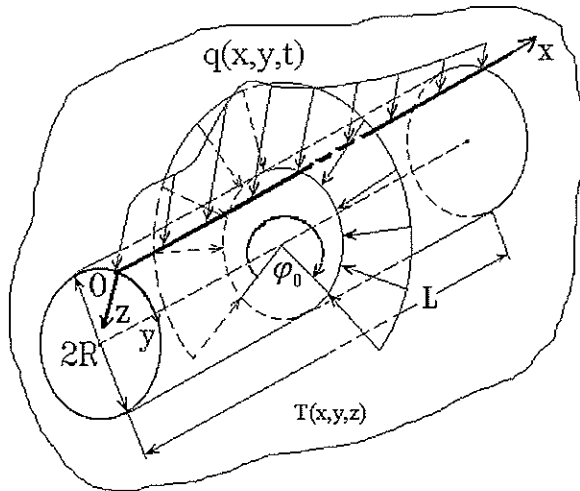


Fig. 1. Computation scheme.

$$\left\{ \lambda^{-2} \frac{\partial^4 F}{\partial x^4} + 2 \frac{\partial^4 F}{\partial x^2 \partial y^2} + \lambda^2 \frac{\partial^4 F}{\partial y^4} + \frac{1}{2} L(w, w) + k_y \frac{\partial^2 w}{\partial x^2} + \lambda^{-1} \frac{\partial^2 N_t}{\partial x^2} + \lambda \frac{\partial^2 N_t}{\partial y^2} \right\} = 0. \quad (1)$$

The following nondimensional parameters are introduced (with the bars):

$$w = 2h\bar{w}, \quad F = E_0(2h)^3 \bar{F}, \quad t = \frac{RL}{2h\sqrt{gE_0}} \bar{t},$$

$$\lambda = \frac{L}{R}; \quad x = L\bar{x}, \quad y = R\bar{y}; \quad k_y = \bar{k}_y \frac{h}{R^2},$$

$$q = \bar{q} \frac{E_0(2h)^4}{L^2 R^2},$$

where  $L$  and  $R = R_y$  are the shell length and radius, respectively,  $t$  denotes time,  $\varepsilon$  is the damping coefficient of a medium where the shell is embedded,  $F$  is the stress (Airy's) function,  $w$  denotes deflection,  $h$  is the shell thickness,  $\nu$  is Poisson's coefficient,  $E_0$  is the Young modulus,  $q(x, y, t)$  is the transversal load,  $k_y$  is the shell curvature regarding  $y$ .

In addition,

$$L(w, F) = \frac{\partial^2 w}{\partial x^2} \frac{\partial^2 F}{\partial y^2} + \frac{\partial^2 w}{\partial y^2} \frac{\partial^2 F}{\partial x^2} - 2 \frac{\partial^2 w}{\partial x \partial y} \frac{\partial^2 F}{\partial x \partial y},$$

$$L(w, w) = 2 \left[ \frac{\partial^2 w}{\partial x^2} \frac{\partial^2 w}{\partial y^2} - \left( \frac{\partial^2 w}{\partial x \partial y} \right)^2 \right]$$

are the known nonlinear operators,  $N_t = (1/h) \times \int_{-\frac{h}{2}}^{\frac{h}{2}} Q dz$  is the temperature-induced force,  $M_t = (12/h^3) \int_{-\frac{h}{2}}^{\frac{h}{2}} Q z dz$  is the temperature-induced torque,  $Q(x, y, z) = T - T_0$  is the temperature increment, whereas  $T_0$  is the initial temperature.



Fig. 2. Support along shell end faces with additional flexible ribs (boundary conditions (2)).

For brevity of our considerations bars over the non-dimensional quantities in Eq. (1) are omitted.

In this work, vibrations of a simple supported shell with the following homogeneous boundary conditions

$$w = 0; \quad \frac{\partial^2 w}{\partial x^2} = 0; \quad F = 0; \quad (2)$$

$$\frac{\partial^2 F}{\partial x^2} = 0 \quad \text{for } x = 0, 1,$$

and with the following initial conditions:

$$w(x, y)|_{t=0} = 0; \quad \frac{\partial w}{\partial t} \Big|_{t=0} = 0 \quad (3)$$

are studied. The physical meaning of the boundary condition of the stress function  $F$  is shown in Fig. 2.

The temperature field  $T$  is given in the following form:  $T(x, y) = C \sin(\pi x) \sin(\pi y)$ . The analytical form of the temperature field distribution satisfies the well-known Poisson equation and it influences the earlier explicitly given temperature-induced force and torque.

Let us consider the dissipative system ( $\varepsilon \neq 0$ ) subjected to transversal loading distributed in zone  $0 \leq \varphi \leq \varphi_0$ ,  $0 \leq x \leq 1$  and being changed harmonically  $q(t) = q_0 \sin(\omega_p t)$ , where  $q_0$  and  $\omega_p$  are the amplitude and frequency of the exciting force, respectively.

### 3. The Bubnov-Galerkin Method and Fourier Representation

The boundary value problem regarding space coordinates is solved by the Bubnov-Galerkin method in higher approximations. Functions  $w$  and  $F$  being solutions to Eqs. (1) are approximated by an expression which consists of the product of functions depending on time and coordinates of the following form

$$w = \sum_{i=0}^{N_1} \sum_{j=0}^{N_2} A_{ij}(t) \varphi_{ij}(x, y), \quad (4)$$

$$F = \sum_{i=0}^{N_1} \sum_{j=0}^{N_2} B_{ij}(t) \psi_{ij}(x, y).$$

In order to find approximated values of functions  $w$  and  $F$  we take the coordinate systems of functions of the form  $\{\varphi_{ij}(x, y), \psi_{ij}(x, y)\}$  ( $i, j = 0, 1, 2, \dots$ ) in (4), which satisfy the following requirements:

- (1)  $\varphi_{ij}(x, y) \in H_A, \psi_{ij}(x, y) \in H_A$ , where  $H_A$  is the Hilbert space, which is further referred to as the energy space.
- (2)  $\forall i, j$  functions  $\varphi_{ij}(x, y)$  and  $\psi_{ij}(x, y)$  are linearly independent and continuous in space  $\Omega$ , together with their derivatives up to the fourth order.
- (3)  $\varphi_{ij}(x, y)$  and  $\psi_{ij}(x, y)$  satisfy rigorously the main boundary conditions (and initial conditions if any).
- (4)  $\varphi_{ij}(x, y)$  and  $\psi_{ij}(x, y)$  satisfy a completeness property in  $H_A$ .
- (5)  $\varphi_{ij}(x, y)$  and  $\psi_{ij}(x, y)$  should represent the first  $N$  elements of the complete system of functions.

The coefficients  $A_{ij}(t)$  and  $B_{ij}(t)$  are the functions of time being sought. For convenience, left-hand sides of Eqs. (1) appearing in brackets are denoted by  $\Phi_1$  and  $\Phi_2$ , and therefore (1) takes the following form:

$$\begin{aligned} \Phi_1 \left( w, F, \frac{\partial^2 w}{\partial x^2}, \frac{\partial^2 F}{\partial x^2}, \dots; M_t, \frac{\partial^2 M_t}{\partial x^2}, \frac{\partial^2 M_t}{\partial y^2} \right) \\ + k_y^2 q(x, y, t) = 0, \\ \Phi_2 \left( w, F, \frac{\partial^2 w}{\partial x^2}, \frac{\partial^2 F}{\partial x^2}, \dots; N_t, \frac{\partial^2 N_t}{\partial x^2}, \frac{\partial^2 N_t}{\partial y^2} \right) \\ = 0. \end{aligned} \tag{5}$$

Applying the Bubnov–Galerkin procedure to (5) one gets

$$\begin{aligned} \int_0^1 \int_0^\xi \Phi_1 \varphi_{kl}(x, y) dx dy \\ + \int_{x_1}^{x_2} \int_{y_1}^{y_2} k_y^2 q(x, y, t) \varphi_{kl}(x, y) dx dy = 0, \\ \int_0^1 \int_0^\xi \Phi_2 \psi_{kl}(x, y) dx dy = 0, \quad k = 0, 1, \dots, N_1; \\ l = 0, 1, \dots, N_2. \end{aligned} \tag{6}$$

Now and further we take  $\xi = 2\pi$  for a closed cylindrical shell. Owing to (6) Eqs. (5) take the following form

$$\begin{aligned} \sum_{kl} \left[ \sum_{ij} A_{ij} S_{ijrskl} + \sum_{ij} B_{ij} C_{1,ijkl} + k_y^2 Q_{kl} + H_{1kl} \right. \\ \left. - \sum_{ij} A_{ij} \sum_{rs} B_{rs} D_{1,ijrskl} \right] \\ - \sum_{ij} \left[ \frac{d^2 A_{ij}}{dt^2} + \varepsilon \frac{dA_{ij}}{dt} \right] G_{ijkl} = 0, \tag{7} \\ \sum_{kl} \left[ \sum_{ij} A_{ij} C_{2,ijkl} + \sum_{ij} B_{ij} \sum_{rs} P_{ijrskl} \right. \\ \left. + \sum_{ij} A_{ij} \sum_{rs} A_{rs} D_{2,ijrskl} + H_{2kl} \right] = 0. \end{aligned}$$

Symbol  $\sum_{kl}[*]$  standing before every equation in system (7) means that each of these equations is understood as the system of  $kl$  equations of these types, and the associated Bubnov–Galerkin integrals have the following form

$$\begin{aligned} S_{ijrskl} &= \int_0^1 \int_0^\xi \frac{1}{12(1-\nu^2)} \left[ \frac{1}{\lambda^2} \frac{\partial^2 \varphi_{ij}}{\partial x^2} \frac{\partial^2 \varphi_{rs}}{\partial x^2} + \lambda^2 \frac{\partial^2 \varphi_{ij}}{\partial y^2} \frac{\partial^2 \varphi_{rs}}{\partial y^2} + 2 \frac{\partial^2 \varphi_{ij}}{\partial x \partial y} \frac{\partial^2 \varphi_{rs}}{\partial x \partial x} \right] \varphi_{kl} dx dy, \\ C_{1,ijkl} &= \int_0^1 \int_0^\xi \left[ -k_y \frac{\partial^2 \psi_{ij}}{\partial x^2} \right] \varphi_{kl} dx dy, \quad C_{2,ijkl} = \int_0^1 \int_0^\xi \left[ k_y \frac{\partial^2 \varphi_{ij}}{\partial x^2} \right] \psi_{kl} dx dy, \\ D_{1,ijrskl} &= \int_0^1 \int_0^\xi L(\varphi_{ij}, \psi_{rs}) \varphi_{kl} dx dy, \quad D_{2,ijrskl} = \int_0^1 \int_0^\xi \frac{1}{2} L(\varphi_{ij}, \varphi_{rs}) \psi_{kl} dx dy, \\ P_{ijrskl} &= \int_0^1 \int_0^\xi \left[ \frac{1}{\lambda^2} \frac{\partial^2 \psi_{ij}}{\partial x^2} \frac{\partial^2 \psi_{rs}}{\partial x^2} + \lambda^2 \frac{\partial^2 \psi_{ij}}{\partial y^2} \frac{\partial^2 \psi_{rs}}{\partial y^2} + 2 \frac{\partial^2 \psi_{ij}}{\partial x \partial y} \frac{\partial^2 \psi_{rs}}{\partial x \partial x} \right] \psi_{kl} dx dy, \\ G_{ijkl} &= \int_0^1 \int_0^\xi \varphi_{ij} \psi_{kl} dx dy, \quad Q_{kl} = \int_0^1 \int_0^\xi \varphi_{kl} q(x, y, t) dx dy, \end{aligned}$$

$$H_{1kl} = \int_0^1 \int_0^\xi \frac{1}{12(1-\nu^2)} \left[ \lambda^{-1} \frac{\partial^2 M_t}{\partial x^2} + \lambda \frac{\partial^2 M_t}{\partial y^2} \right] \varphi_{kl} dx dy, \tag{8}$$

$$H_{2kl} = \int_0^1 \int_0^\xi \left[ \lambda^{-1} \frac{\partial^2 N_t}{\partial x^2} + \lambda \frac{\partial^2 N_t}{\partial y^2} \right] \psi_{kl} dx dy.$$

Integrals (8), except of  $Q_{kl}$  corresponding only to the part of the shell area, are computed regarding the whole shell surface. After application of the Bubnov–Galerkin procedure the obtained system of ordinary differential equations with respect to functions  $A_{ij}(t)$  and  $B_{ij}(t)$  has the following matrix form

$$\begin{aligned} \mathbf{G}(\ddot{\mathbf{A}} + \varepsilon \dot{\mathbf{A}}) + \mathbf{S}\mathbf{A} + \mathbf{C}_1\mathbf{B} + \mathbf{D}_1\mathbf{A}\mathbf{B} &= \mathbf{Q}q(t) + \mathbf{H}_1, \\ \mathbf{C}_2\mathbf{A} + \mathbf{P}\mathbf{B} + \mathbf{D}_2\mathbf{A}\mathbf{A} &= \mathbf{H}_2, \end{aligned} \tag{9}$$

where  $\mathbf{G} = \|G_{ijkl}\|$ ,  $\mathbf{S} = \|S_{ijrskl}\|$ ,  $\mathbf{C}_1 = \|C_{1ijkl}\|$ ,  $\mathbf{C}_2 = \|C_{2ijkl}\|$ ,  $\mathbf{D}_1 = \|D_{1ijrskl}\|$ ,  $\mathbf{D}_2 = \|D_{2ijrskl}\|$ ,  $\mathbf{P} = \|P_{ijkl}\|$  — square matrices of dimension  $2 \cdot N_1 \cdot N_2 \times 2 \cdot N_1 \cdot N_2$ , and  $\mathbf{A} = \|A_{ij}\|$ ,  $\mathbf{B} = \|B_{ij}\|$ ,  $\mathbf{Q} = \|Q_{ij}\|$  are the matrices of dimension  $2 \cdot N_1 \cdot N_2 \times 1$ .

Further, second equation of system (9) is solved regarding matrix  $\mathbf{B}$ , and then it is solved by the method of inverse matrix on each time step:

$$\begin{aligned} \mathbf{B} &= [-\mathbf{P}^{-1}\mathbf{D}_2\mathbf{A} - \mathbf{P}^{-1}\mathbf{C}_2]\mathbf{A} + \mathbf{P}^{-1}\mathbf{H}_2\mathbf{C}_2\mathbf{A} \\ &\quad + \mathbf{P}\mathbf{B} + \mathbf{D}_2\mathbf{A}\mathbf{A} \\ &= \mathbf{H}_2. \end{aligned} \tag{10}$$

Multiplying first equation of (10) by  $\mathbf{G}^{-1}$  and introducing notation  $\dot{\mathbf{A}} = \mathbf{R}$  the following Cauchy problem regarding nonlinear first order ODEs is formulated

$$\begin{cases} \dot{\mathbf{R}} = -\varepsilon\mathbf{R} + \mathbf{G}^{-1}\mathbf{D}_1\mathbf{A}\mathbf{B} - \mathbf{G}^{-1}\mathbf{S}\mathbf{A} \\ \quad + q(\bar{t})\mathbf{G}^{-1}\mathbf{Q} + \mathbf{G}^{-1}\mathbf{H}_1, \\ \dot{\mathbf{A}} = \mathbf{R}. \end{cases} \tag{11}$$

The introduced transformation is allowed since the inversed matrices  $\mathbf{G}^{-1}$  and  $\mathbf{P}^{-1}$  exist if the coordinate functions are linearly independent.

Equations (11) are supplemented by boundary and initial conditions and the obtained Cauchy problem is solved by the fourth order Runge–Kutta method. Step in time is chosen via the Runge rule. Results obtained using various computational methods were compared by Krysko and Narkaytis [2005], who showed that integration by the fourth Runge–Kutta method was sufficient and the application of higher order Runge–Kutta approaches was time consuming and did not yield improvement of the results.

In our case,  $\varphi_{ij}, \psi_{ij}$  in (4) are approximated by the product of two functions, where each depends only on one argument which satisfies boundary conditions (2) and (3):

$$\begin{aligned} w &= \sum_{i=1}^{N_1} \sum_{j=0}^{N_2} A_{ij}(t) \sin(i\pi x) \cos(jy), \\ F &= \sum_{i=1}^{N_1} \sum_{j=0}^{N_2} B_{ij}(t) \sin(i\pi x) \cos(jy). \end{aligned} \tag{12}$$

Integrals of the Bubnov–Galerkin procedure are computed using the following formulas

$$\begin{aligned} I_{1,i} &= \int_0^1 \sin(i\pi x) dx = \begin{cases} 0, & i = 0, 2, 4, \dots \\ \frac{2}{i\pi}, & i = 1, 3, 5, \dots \end{cases}, \\ I_{2,ik} &= \int_0^1 \sin(i\pi x) \sin(k\pi x) dx = \begin{cases} \frac{1}{2}, & i = j, \\ 0, & i \neq j, \end{cases} \\ I_{1,j} &= \int_0^{2\pi} \cos(jy) dy = 0, \\ I_{2,jl} &= \int_0^{2\pi} \cos(jy) \cos(ly) dy = \begin{cases} \frac{1}{4} \left[ \frac{\sin(2\pi\alpha_1)}{\alpha_1} + \frac{\sin(2\pi\alpha_2)}{\alpha_2} \right], & \alpha_z \neq 0, \quad z = 1; \\ \frac{\sin(2\pi\alpha_2)}{\alpha_2} \approx 2\pi, & \alpha_z = 0, \quad z = 1; \end{cases} \end{aligned}$$

$$\begin{aligned}
 I_{3,ikr} &= \int_0^1 \sin(i\pi x) \sin(r\pi x) \sin(k\pi x) dx = \begin{cases} \frac{1}{4\pi} \left[ -\frac{\cos(\beta_1\pi)}{\beta_1} - \frac{\cos(\beta_2\pi)}{\beta_2} - \frac{\cos(\beta_3\pi)}{\beta_3} - \frac{\cos(\beta_4\pi)}{\beta_4} \right. \\ \left. + \frac{1}{\beta_1} + \frac{1}{\beta_2} + \frac{1}{\beta_3} + \frac{1}{\beta_4} \right], & \beta_v \neq 0; \\ \left[ \frac{\cos(\beta_v\pi)}{\beta_v} \approx 0, \frac{1}{\beta_v} \approx 0 \right], & v = 1, 2, 3, & \beta_v = 0; \end{cases} \\
 I_{3,jls} &= \int_0^{2\pi} \cos(jy) \cos(sy) \cos(ly) dy = \begin{cases} \frac{1}{4} \left[ \frac{\sin(2\pi\gamma_1)}{\gamma_1} + \frac{\sin(2\pi\gamma_2)}{\gamma_2} + \frac{\sin(2\pi\gamma_3)}{\gamma_3} + \frac{\sin(2\pi\gamma_4)}{\gamma_4} \right], & \gamma_v \neq 0; \\ \frac{\sin(2\pi\gamma_v)}{\gamma_v} \approx 2\pi, & v = 1, 2, 4 & \gamma_v = 0; \end{cases} \\
 I_{4,ikr} &= \int_0^1 \cos(i\pi x) \cos(r\pi x) \sin(k\pi x) dx = \begin{cases} \frac{1}{4\pi} \left[ \frac{\cos(\beta_1\pi)}{\beta_1} - \frac{\cos(\beta_2\pi)}{\beta_2} - \frac{\cos(\beta_3\pi)}{\beta_3} - \frac{\cos(\beta_4\pi)}{\beta_4} \right. \\ \left. - \frac{1}{\beta_1} + \frac{1}{\beta_2} + \frac{1}{\beta_3} + \frac{1}{\beta_4} \right], & \beta_v \neq 0; \\ \left[ \frac{\cos(\beta_v\pi)}{\beta_v} \approx 0, \frac{1}{\beta_v} \approx 0 \right], & v = 1, 2, 3, & \beta_v = 0; \end{cases} \\
 I_{4,jls} &= \int_0^{2\pi} \sin(jy) \sin(sy) \cos(ly) dy = \begin{cases} \frac{1}{4} \left[ \frac{\sin(2\pi\gamma_1)}{\gamma_1} + \frac{\sin(2\pi\gamma_2)}{\gamma_2} - \frac{\sin(2\pi\gamma_3)}{\gamma_3} - \frac{\sin(2\pi\gamma_4)}{\gamma_4} \right], & \gamma_v \neq 0; \\ \frac{\sin(2\pi\gamma_v)}{\gamma_v} \approx 2\pi, & v = 1, 2, 4 & \gamma_v = 0; \end{cases}
 \end{aligned} \tag{13}$$

where

$$\begin{aligned}
 \alpha_1 &= j + l, & \alpha_2 &= j - l, \\
 \beta_1 &= i + r - k, & \beta_2 &= -i + r + k, & \beta_3 &= i - r + k, & \beta_4 &= i + r + k, \\
 \gamma_1 &= j - s + l, & \gamma_2 &= j - s - l, & \gamma_3 &= j + s + l, & \gamma_4 &= j + s - l.
 \end{aligned}$$

The following notation is further introduced

$$\begin{aligned}
 I_Q^{kl} &= M \cdot I_{1i} I_{1j}, & M &= k_y^2, & I_{AB}^{kl} &= r^2 k_y \pi^2 I_{2,ik} I_{2,jl}, & I_{H_1}^{kl} &= C \frac{2\pi^2}{\lambda} I_{1i} I_{1j}, & I_{H_2}^{kl} &= C 2\pi^2 \lambda I_{1i} I_{1j}, \\
 I_{ijklrs} &= \pi^2 [(i^2 l^2 + j^2 k^2) I_{3ikr} I_{3jls} - 2ijkl I_{4ikr} I_{4jls}], & I_{kl}^t &= I_{2,ik} I_{2,jl}, \\
 J_{1,ijkl}^{kl} &= \frac{\pi^2}{12(1 - \mu^2)} \left[ \frac{r^4}{\lambda^2} + 2r^2 s^2 + \lambda^2 s^4 \right] \cdot I_{2,ir} I_{2,js}, & J_{2,ijkl}^{kl} &= \left[ \frac{r^4}{\lambda^2} + 2r^2 s^2 + \lambda^2 s^4 \right] \cdot \pi^2 I_{2,ir} I_{2,js}.
 \end{aligned}$$

Therefore, taking into account the given integrals, system (11) assumes the form:

$$\sum_{kl} \left\{ \sum_{ij} \sum_{rs} \left[ J_{1,ijkl}^{kl} A_{ij} + I_{AB}^{kl} B_{rs} + I_Q^{kl} q(t) + A_{ij} B_{kl} I_{ijklrs} + \left( \frac{d^2 A_{ij}}{dt^2} + \varepsilon \frac{d A_{ij}}{dt} \right) I_{kl}^t \right] \right\} = 0, \tag{14}$$

$$\sum_{kl} \left\{ \sum_{ij} \sum_{rs} \left[ J_{2,ijkl}^{kl} B_{ij} + I_{AB}^{kl} A_{rs} + I_{H_1}^{kl} + I_{H_2}^{kl} + \frac{1}{2} A_{ij} A_{kl} I_{ijklrs} \right] \right\} = 0. \tag{15}$$

The Bubnov–Galerkin algorithm described briefly so far allows a wide class of problems, both static and dynamic, to be solved. A solution to static problems is obtained via the method first applied by Feodos'ev (the so-called “set up method”) [Feodos'ev, 1963], and widely applied for instance, in a monograph by Awrejcewicz and Krysko [2003]. In order to solve static problems of plates and shells, various approximate methods have been applied allowing the partial differential equations to be reduced to the system of nonlinear algebraic equations, which is usually further linearized. In the set-up method a solution to PDEs is reduced to that of the Cauchy problem of ODEs.

Equation (15) is solved regarding matrix  $B$ . Then, substituting found coefficients  $B_{kl}$  into (14) one gets second order ODEs with respect to  $A_{kl}$ , which are solved using the fourth order Runge–Kutta method.

#### 4. Numerical Example

Next, we study the dynamic behavior of the circular closed shell defined by parameters  $k_y = 112.5$ ,  $\lambda = 2$ ,  $\varepsilon = 9$  embedded into a temperature field and transversally loaded by  $q(t) = q_0 \sin(\omega_p t)$  acting on the shell surface  $0 \leq \varphi \leq 1, 9\pi$ ,  $0 \leq x \leq 1$  for the case of  $\omega = \omega_p = 26.176$ . First, an influence of the series number of approximating functions on the solution is analyzed for  $N_2 = 7$  and  $N_2 = 9$ . Space distributed vibrations of the shell are studied for  $0 \leq x \leq 1; 0 \leq y \leq 2\pi$ , whereas shell cross-sections are analyzed for  $x = 0.5; 0 \leq y \leq 2\pi$  for  $N_2 = 7$  and  $N_2 = 9$ . In addition, heat influence on the shell stress-strain state is traced via monitoring of the shell deflection surface, stresses and bending torque distributions for temperature amplitudes  $C = 0$  and  $C = 50$ . Simultaneously, the relation  $w_{\max}(C)$  is monitored for fixed amplitude

$q_0$ , as well as the relation  $w_{\max}(q_0)$  for fixed excitation frequency  $\omega_p = \omega_0$ , where  $\omega_0$  is the fundamental frequency of shell linear vibrations. Finally, the so-called scales of shell vibration type are constructed. Investigation of the function  $w_{\max}(C)$  for each  $C$  enables determination of instability zones of the shell subjected to the temperature field. The constructed scales of shell vibrations make it possible to study easily the shell dynamic behavior including transition scenarios from regular to chaotic dynamics, as well as to estimate a critical set of the shell parameters, where a further shell heating is impossible, since it causes its destruction. Let us study a stabilization process of the shell chaotic vibrations as well as its stability loss versus parameter  $C$ . For this purpose the relation  $w_{\max}(q_0)$  is monitored for every fixed value of  $C$  and the relation  $w_{\max}(C)$  is studied for some fixed values of  $q_0$ . This approach provides the estimation of stability zones and enables all fundamental shell dynamic characteristics to be established at some control points of the shell pre- and post-critical states.

Let us fix the frequency of excitation  $\omega_p = \omega_0 = 26.176$  and let us construct vibration scales using the observation of a frequency power spectrum. A given scale represents part of the shell vibration chart. Namely, it represents a narrow band of the chart regarding frequency  $\omega_p = 26.176$  versus load amplitude  $q_0$ . Figure 3 shows the scales of the shell dynamic regime regarding variation of the excitation amplitude  $0 \leq q_0 \leq 0.4$ . On the other hand, Fig. 3(a) illustrates a corresponding scale regarding lack of the temperature field ( $C = 0$ ). Furthermore, Fig. 3(b) refers to  $C = 10$ , whereas Fig. 3(c) refers to  $C = 50$ . When analyzing the mentioned figures, one may conclude that a simultaneous increase of both amplitudes of temperature and excitation causes a decrease of the periodic behavior. Namely, chaotic zones are increased and

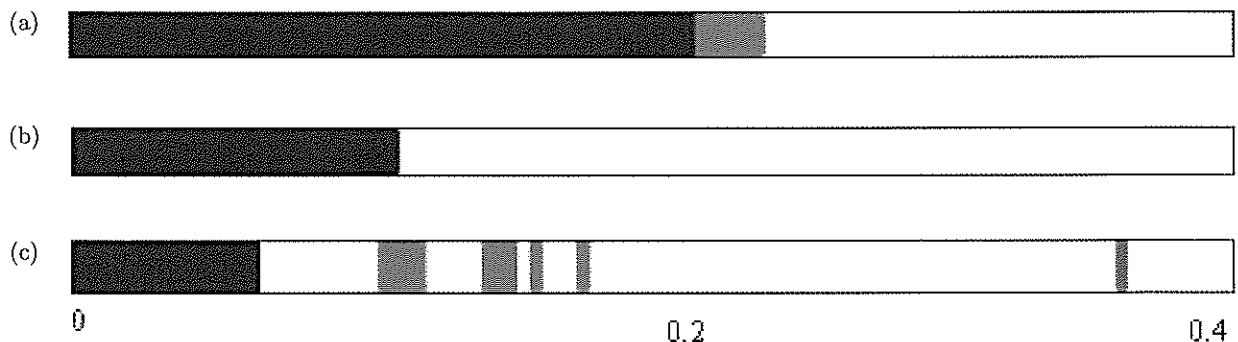


Fig. 3. Vibration scales versus amplitude  $q_0$ .



the transition scenarios associated with bifurcation zones do not appear, although zones regarding the superposition of frequencies are observed.

The values of  $q_0$  of zones shown in Fig. 3(a) are chosen in the following way: harmonic zone —  $q_0 = 0.1$ ; frequencies superposition zone —  $q_0 = 0.24$ , and chaotic zone —  $q_0 = 0.3$ . Then the shell dynamics is studied for fixed  $q_0$  and for the variation of  $0 \leq C \leq 50$ . The corresponding drawings and scales characterizing the shell behavior for the given conditions are reported in Fig. 4, where the relation  $w_{\max}(C)$  and scales of the dynamic regimes are constructed for  $N_2 = 7$ .

Note that the system exhibits sudden jumps, i.e. the shell passes through various dynamic states. For instance for  $q_0 = 0.1$  for  $C = 39.71$  (point **A2**) a sudden jump is observed, and although one may achieve convergence in average power spectrum regarding frequency, but a number of series terms approximating a solution plays a crucial role in the estimation of the shell stress-strain state. Below, we study the shell deflection form as well as the forms of transversal shell cross-sections for fixed temperature and loading in the neighborhood of a jump and for its maximal value. Table 1 gives the shell cross-sections for fixed time instants and for

fixed value of  $x = 0.5$  and for  $0 \leq y \leq 2\pi$ . The forms of transversal cross-sections ( $x = 0.5; y \in [0; 2\pi]$ ) are studied for the same time instants. The reported wave forms of the circular shell refer to points **A1** and **A2** and they are shown in Fig. 4, whereas the shell points **B1**, **B2** correspond to graph 2 in Fig. 4.

The cross-section I-I has been obtained in the following way: the shell cylindrical surface is cut by a plane going over the cylinder axis and dividing the surface into two parts.

For comparison of the shell dynamics at points **A1** and **A2** (see curve 1 in Fig. 4) the shell deflections and the shell transversal cross-sections are analyzed using the following characteristics: time history  $w(t; x_0; y_0)$ , phase portrait  $w(w')$ , power spectrum  $S(\omega)$ , and Poincaré map  $w_t(w_{t+T})$ . For instance, the system state shown in scale 1 of Fig. 4 is recognized as periodic, which is manifested by the already mentioned characteristics. The maximal shell deflection occurs in the zones situated in the neighborhood of the borders of externally loading zone as well as inside it. The existence of a temperature field causes not only an increase of the shell deflection, but also its buckling. However, in the case of the shell behavior exhibited by point

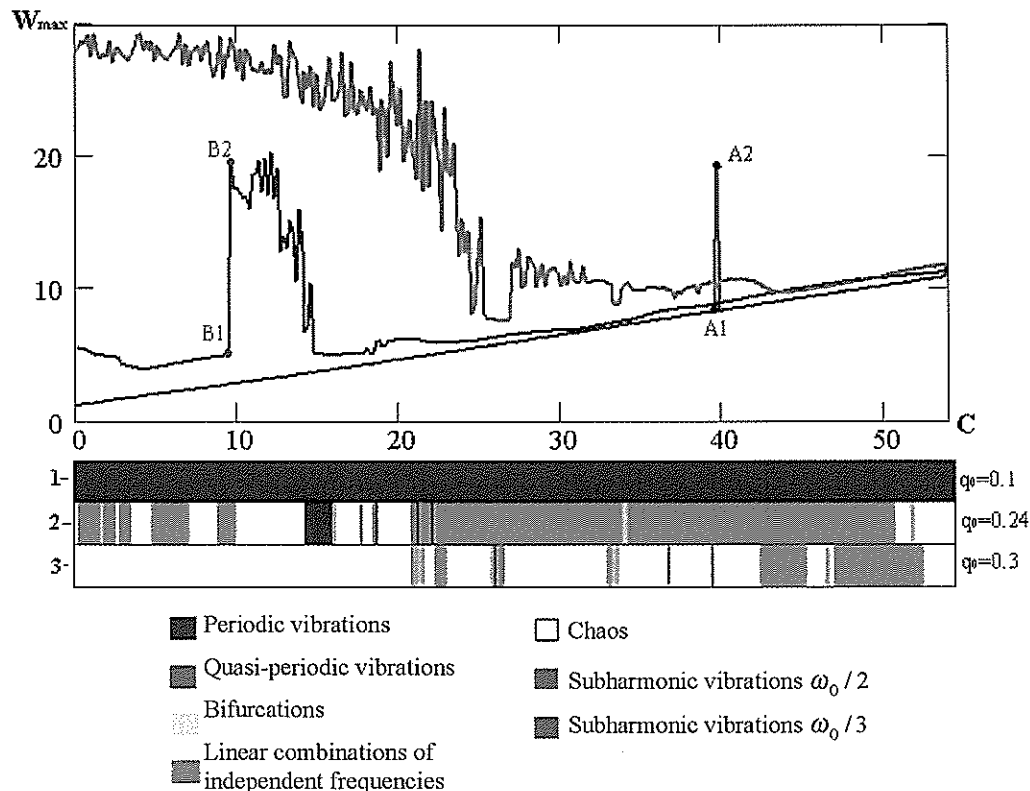
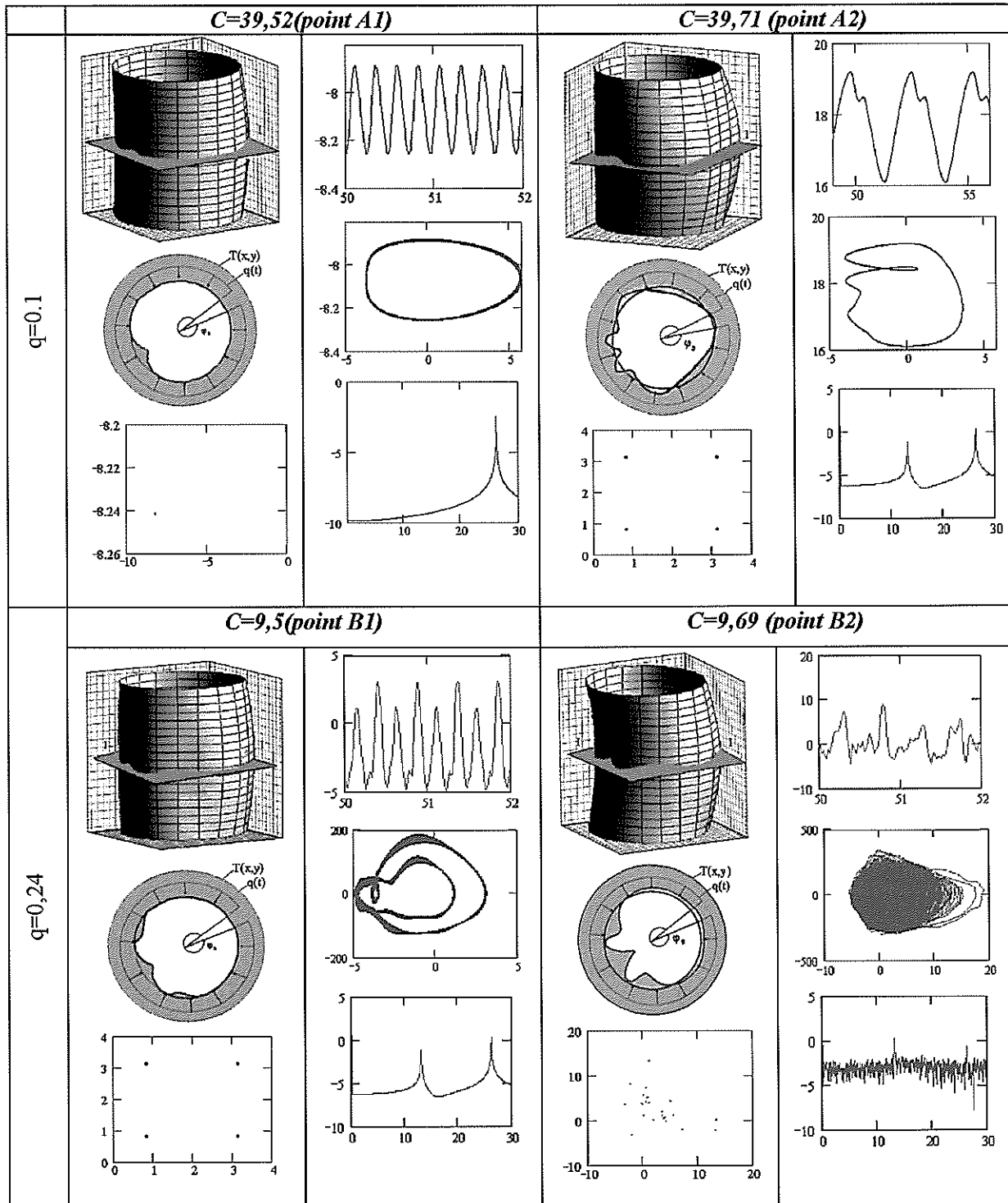


Fig. 4. Functions  $w_{\max}(C)$  and scales of dynamic regimes of the shell for  $N_2 = 7$ .

Table 1.



A2, the shell deflection is rapidly changed and in both time history and phase portrait, two-frequency vibrations occur. Note, that the system still exhibits periodic behavior, although a crucial role is played here by a number of solution terms, which will be shown for the same parameter  $C = 39, 71$ , but for the series terms number  $N_2 = 9$ .

Note, that in the case of transversal shell cross-section at points B1 and B2 a similar shell bending form is observed, whereas at point B2 one may observe large chaotic shell deflections. Owing to observed four points in the Poincaré cross-section at point B1 and the corresponding two loops in the phase portrait, one may detect a Hopf bifurcation.

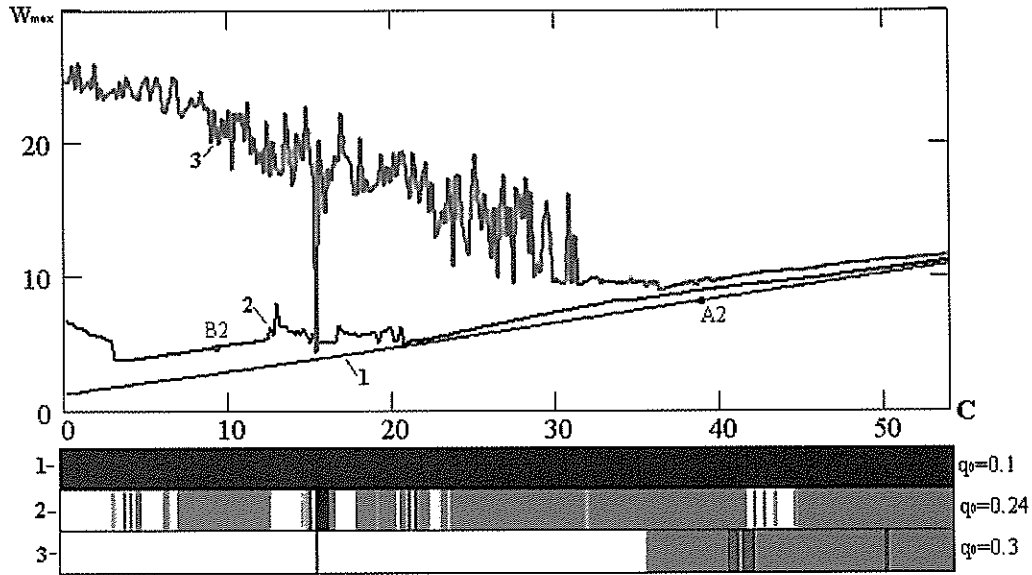


Fig. 5. Relation  $w_{max}(q_0)$  and scales of dynamic regimes for  $N_2 = 9$ .

Next, we study the shell deflection forms and the shell transversal cross-section forms for the number of terms used in approximation  $N_2 = 9$ .

Comparing the graphs in Figs. 4 and 5 for points A2 and B2, respectively, one may observe that the vibration process depends essentially on

the number of terms used in the approximating real solution series (the results reported further are obtained for  $N_2 = 9$ ). The shell deflection forms and the shell transversal cross-section forms together with the fundamental characteristics regarding points A2 and B2 are reported in Table 2.

Table 2.

| $C=39,71$ (point A2), $q=0.1$ |  | $C=9,69$ (point B2), $q=0.24$ |  |
|-------------------------------|--|-------------------------------|--|
|                               |  |                               |  |
|                               |  |                               |  |
|                               |  |                               |  |

Note that at point **A2** for  $C = 39.71$ , contrary to the case associated with  $N_2 = 7$ , a stabilization of the vibration process occurs towards regularity of the shell dynamics. Besides, a transition from chaos to quasi-periodic vibration is observed in the case corresponding to point **B2**. Owing to the results shown in Fig. 5, one may conclude that the shell dynamics tends to be a regular process for  $C \geq 50$ .

In order to get a possible full picture of the shell behavior for a given time instant, it is required to investigate the shell stress-strain states. The

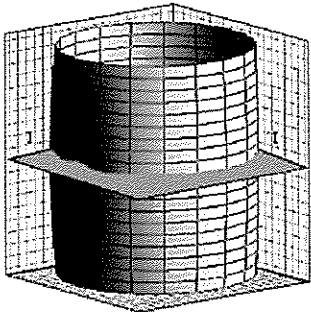
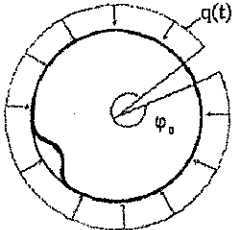
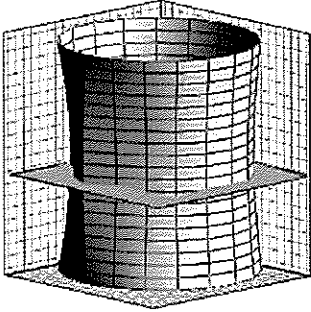
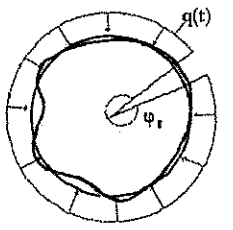
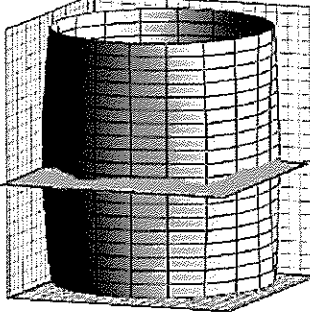
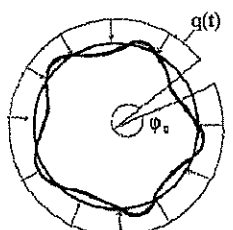
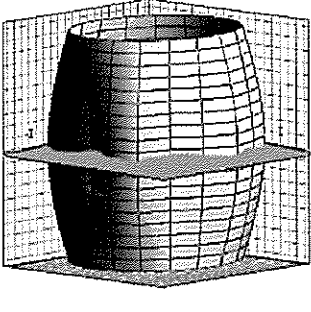
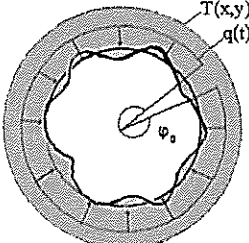
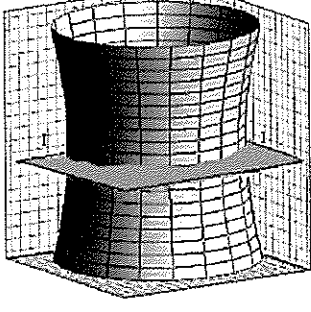
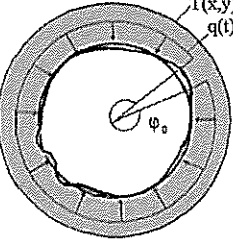
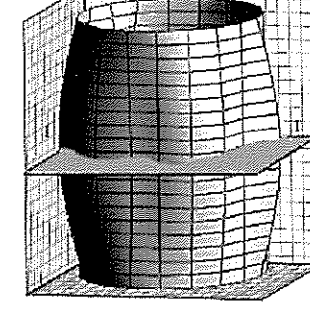
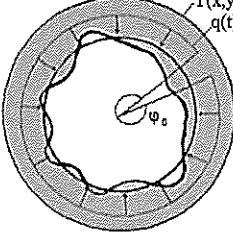
bending torques are governed by the following equations:

$$M_x = - \left( \frac{\partial^2 w}{\partial x^2} + \nu \frac{\partial^2 w}{\partial y^2} \right),$$

$$M_y = - \left[ \frac{\partial^2 w}{\partial y^2} + \nu \frac{\partial^2 w}{\partial x^2} \right].$$

The shell deflection forms and the shell transversal cross-sections for the bending torque  $M^* = M_x + M_y$  and for the stress function  $F_n = (\partial^2 F / \partial x^2) + (\partial^2 F / \partial y^2)$  are given in Table 3.

Table 3.

|      | $w(t, x_0, y_0)$   | $F_n$  | $M^*$  |
|------|--|--|--|
| C=0  |  <p>section I-I</p>   |  <p>section I-I</p>   |  <p>section I-I</p>   |
| C=50 |  <p>section I-I</p>  |  <p>section I-I</p>  |  <p>section I-I</p>  |

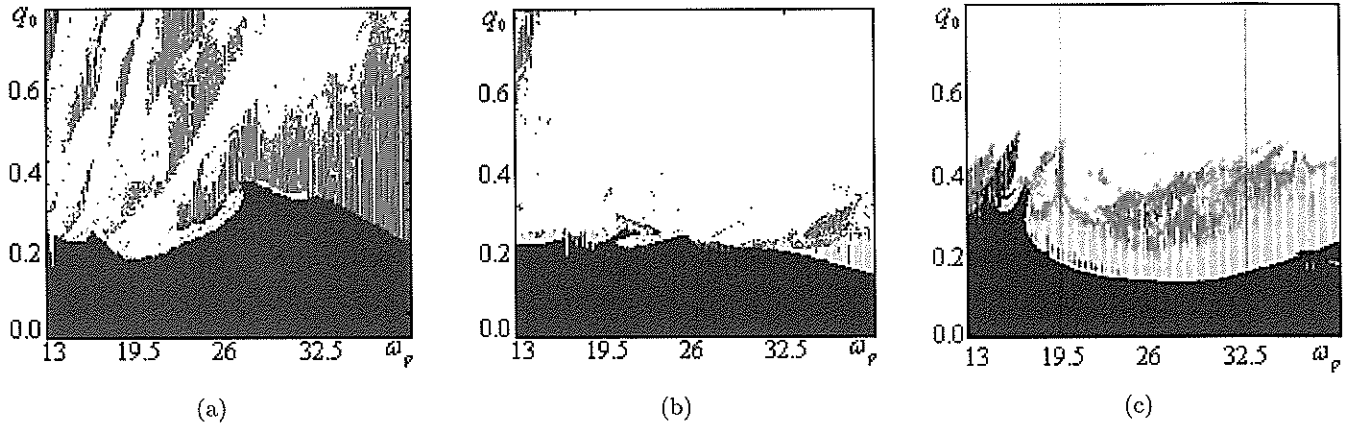


Fig. 6. Charts of shell dynamic regimes in plane  $\{q_0, \omega_p\}$ .

Note, that when the temperature field is not activated ( $C = 0$ ), one may observe the shell indentation in the neighborhood of the area of external loading action. Increasing the temperature amplitude action ( $C = 50$ ), the shell deflection increases in the zones of both loading and temperature actions and the shell stress-strain state is more activated. Deformation waves are propagated into the whole shell surface yielding increase of the shell deflection. One large and a few small dents are observed in the middle shell surface owing to the stress function analysis. However, analysis of the bending torque exhibits waves propagated on the whole shell surface. On the other hand, for  $C = 50$ , a qualitative change in the shell middle surface is observed since it is buckled in the vicinity of the load  $q(t)$  action. The stress function exhibits both intensive dents and convex buckling in the neighborhood of load action.

Although in this work our aim was to study chaotic shell dynamics, the engineers were interested in getting information of the full shell behavior regarding variation of the external load parameters. For this reason the so-called charts of the vibration shell behavior versus control parameters (here temperature amplitude and external load amplitude and frequency) are constructed. A chart represents the parameters plane  $(q_0, \omega_p)$ , where the temperature amplitude  $C$  is additionally changed. Each point of a chart possesses its own color corresponding to the shell vibration regime. In other words one gets the system dynamics presented in a condensed matter. Numerical computations are carried out for  $N_1 = 1$ ,  $N_2 = 7$ , and a set of parameters  $(q_0, \omega_p)$  is covered by the mesh of  $300 \times 300$  points. Namely, a number of problems being solved achieves

the value of  $9 \cdot 10^4$ . Each of the mentioned problems has been studied using the qualitative theories of differential equations and nonlinear dynamics. The frequency power spectra, phase portraits, Lyapunov exponents, time histories and the Poincaré sections are monitored.

Three charts are shown in Fig. 6. Figure 6(a) is associated with the lack of temperature action ( $C = 0$  in formula  $T(x, y) = C \sin(\pi x) \sin(\pi y)$ ), whereas Fig. 6b(c) corresponds to  $C = 10$  ( $C = 50$ ).

It should be emphasized that the chart undergoes essential changes when the temperature amplitude increases. Zones of regular shell dynamics are similar only for small values of  $0 \leq q_0 \leq 0.2$  and the shell exhibits periodic dynamics. However, for  $q_0 \geq 0.2$  and for  $C = 10$ , the shell exhibits chaotic dynamics. The monitored shell stress-strain characteristics indicate that the shell deflections increase and large dents occurrence is observed. On the other hand, for  $C = 50$  large bifurcation zones appear.

## 5. Concluding Remarks

A novel computational approach to the solving of strongly nonlinear partial differential equations by modeling the dynamics of closed circular shells using the Bubnov-Galerkin approach modified by Vlasov is presented in this paper. It has been shown that both shell vibration character and accuracy of the obtained results depend strongly on the number of terms used in the series approximating the sought solution.

Next, the main results are briefly summarized. The influence of external temperature field together with the band type time-changing load applied in

the interval of  $0 \leq \varphi \leq 1,9\pi$  causes an increase of the shell chaotic dynamics (see Figs. 3(b) and 3(c)). The increase of the loading surface causes an increase of the chaotic zones ( $q_0 \geq 0.4$ ), and also the Hopf bifurcation zones increase substantially.

The shell stress-strain state is characterized by the increase of the shell deflections and the wave propagations are exhibited by the shell middle surface.

## References

- Amabili, M., Pellicano, F. & Païdoussis, M. P. [1998] "Non-linear vibrations of simply supported circular cylindrical shells coupled to quiescent fluid," *J. Fluids Struct.* **12**, 883–918.
- Amabili, M. [2005] "Non-linear vibrations of doubly curved shallow shells," *Int. J. Non-Lin. Mech.* **40**, 683–710.
- Avduevskiy, V. S., Galitseyskiy, B. M. & Glebov, G. A. [1992] *Introduction to Heat Transfer in Airplanes and Rocket-Cosmic Techniques*, eds. Avduevskiy, Koshkin, Mashinostroyeniye, Moscow (in Russian).
- Awrejcewicz, J. & Krysko, V. A. [2003a] *Nonclassical Thermoelastic Problem in Nonlinear Dynamics of Shells* (Springer-Verlag, Berlin).
- Awrejcewicz, J. & Krysko, A. V. [2003b] "Analysis of complex parametric vibrations of plates and shells using Bubnov-Galerkin approach," *Arch. Appl. Mech.* **73**, 495–504.
- Awrejcewicz, J., Krysko, V. A. & Shchekaturova, T. V. [2005] "Transitions from regular to chaotic vibrations of spherical and conical axially-symmetric shells," *Int. J. Struct. Stab. Dyn.* **5**, 359–385.
- Awrejcewicz, J., Krysko, V. A. & Krysko, A. V. [2007] *Thermo-Dynamics of Plates and Shells* (Springer-Verlag, Berlin).
- Bakulin, V. N., Obratsov, I. F. & Potopakhin, V. A. [1998] *Dynamical Problems of Theory of Composite Shells, Influence of Thermo-Dynamic Loads and Concentrated Energy Flows* (Moscow, FizMatLit) (in Russian).
- Benamar, R., Bennouna, M. M. K. & White, R. G. [1994] "The effects of large vibration amplitudes on the mode shapes and natural frequencies of thin elastic structures," *J. Sound Vibr.* **175**, 377–395.
- Bolotin, V. V. [1964] *The Dynamic Stability of Elastic Systems* (Holden-Day, San Francisco).
- Chang, S. I., Lee, J. M., Bajaj, A. K. & Krousgrill, C. M. [1997] "Subharmonic responses in harmonically excited rectangular plates with one-to-one internal resonance," *Chaos Solit. Fract.* **8**, 479–498.
- Cheng, C.-J. & Fan, X.-J. [2001] "Nonlinear mathematical theory of perforated viscoelastic thin plates with its applications," *Int. J. Solids Struct.* **38**, 6627–6641.
- Evensen, D. A. [1974] "Non-linear vibrations of circular cylindrical shells," *Thin Walled Structures: Theory, Experiment and Design*, eds. Fung, Y. C. & Sechler, E. E. (Prentice-Hall, Englewood Cliffs, NY), pp. 133–155.
- Feodos'ev, V. I. [1963] "On the method of solution of stability of deformable systems," *Prikladnaya Matematika i Mekhanika* **27**, 265–275 (in Russian).
- Guo, X. & Mei, C. [2006] "Application of aeroelastic modes on nonlinear supersonic panel flutter at elevated temperatures," *Comp. & Struct.* **84**, 1619–1628.
- Krysko, V. A. & Narkaytis, G. G. [2005] "Comparison of various computational methods using example of vibration modelling of flexible infinite plates subjected to sign changeable loads," *Proc. XXI Int. Conf. Plate and Shell Theories*, Saratov, pp. 281–288.
- Lai, H.-Y., Chen, C.-K. & Yeh, Y.-L. [2002] "Double-mode modeling of chaotic and bifurcation dynamics for a simply supported rectangular plate in large deflection," *Int. J. Non-Lin. Mech.* **37**, 331–343.
- Leissa, A. W. [1973], *Vibration of Shells*, Report NASA SP-288, Government Printing Office, Washington, DC.
- Liew, K. M., Lim, C. W. & Ong, L. S. [1994] "Flexural vibration of doubly-tapered cylindrical shallow shells," *Int. J. Mech. Sci.* **36**, 547–565.
- Murphy, K. D., Virgin, L. N. & Rizzi, S. A. [1996] "Characterizing the dynamic response of a thermally loaded, acoustically excited plate," *J. Sound Vibr.* **196**, 635–658.
- Nagai, K., Maruyama, S., Oya, M. & Yamaguchi, T. [2004] "Chaotic oscillations of a shallow cylindrical shell with a concentrated mass under periodic excitation," *Comp. Struct.* **82**, 2607–2619.
- Nayfeh, H. & Mook, D. T. [1979] *Non-linear Oscillations* (Wiley, NY).
- Païdoussis, M. P. & Li, G. X. [1992] "Cross-flow-induced chaotic vibrations of heat-exchanger tubes impacting on loose supports," *J. Sound Vibr.* **152**, 305–326.
- Pellicano, F. & Amabili, M. [2006] "Dynamic instability and chaos of empty and fluid-filled circular cylindrical shells under periodic axial loads," *J. Sound Vibr.* **293**, 227–252.
- Popov, A. A., Thompson, J. M. T. & McRobie, F. A. [2001] "Chaotic energy exchange through auto-parametric resonance in cylindrical shells," *J. Sound Vibr.* **248**, 395–411.
- Raouf, R. A. & Nayfeh, A. H. [1990] "Non-linear axisymmetric response of closed spherical shells to a radial harmonic excitation," *Int. J. Non-Lin. Mech.* **25**, 475–492.
- Ribeiro, P. & Duarte, R. P. [2006] "From periodic to chaotic oscillations in composite laminated plates," *Comp. Struct.* **84**, 1629–1639.

- Ribeiro, P. [2007] "Thermally induced transitions to chaos in plate vibrations," *J. Sound Vibr.* **299**, 314–330.
- Ross, C. T. F. [1975] "Finite elements for the vibration of cones and cylinders," *Int. J. Num. Meth. Eng.* **9**, 833–845.
- Sheng, D.-F. & Cheng, C.-J. [2004] "Dynamical behaviors of nonlinear viscoelastic thick plates with damage," *Int. J. Solids Struct.* **41**, 7287–7308.
- Soliman, M. S. & Goncalves, P. B. [2003] "Chaotic behavior resulting in transient and steady state instabilities of pressure-loaded shallow spherical shells," *J. Sound Vibr.* **259**, 497–512.
- Sun, Y. X. & Zhang, S. Y. [2001] "Chaotic dynamic analysis of viscoelastic plates," *Int. J. Mech. Sci.* **43**, 1195–1208.
- Thomson, J. M. T. & Bishop, S. R. [1994] *Non-Linearity and Chaos in Engineering Dynamics*, Centre for Non-linear Dynamics, (John Wiley & Sons, NY).
- Volmir, A. S. [1963] *Stability of Elastic Systems* (in Russian) (Moscow, Fizmatgiz).
- Volmir, A. S. [1972] *Nonlinear Dynamics of Plates and Shells* (in Russian) (Nauka, Moscow).
- Xiao, Y.-G., Fu, Y.-M. & Zha, X.-D. [2008] "Bifurcation and chaos of rectangular moderately thick cracked plates on an elastic foundation subjected to periodic load," *Chaos Solit. Fract.* **35**, 460–465.
- Yang, X. L. & Sethna, P. R. [1992] "Non-linear phenomena in forced vibrations of a nearly square plate: Antisymmetric case," *J. Sound Vibr.* **155**, 413–441.